Correlation of microwave dielectric properties and normal vibration modes of $x\mathrm{Ba}(\mathrm{Mg}_{1/3}\mathrm{Ta}_{2/3})\mathrm{O}_3-(1-x)\mathrm{Ba}(\mathrm{Mg}_{1/3}\mathrm{Nb}_{2/3})\mathrm{O}_3$ ceramics: II. Infrared spectroscopy

Yi-Chun Chen, Hsiu-Fung Cheng, Hsiang-Lin Liu, and Chih-Ta Chia[a)]
Department of Physics, National Taiwan Normal University, Taipei, Taiwan 116, Republic of China

I-Nan Lin
Materials Science Center, National Tsing-Hua University, Hsinchu, Taiwan 300, Republic of China

(Received 11 February 2003; accepted 9 June 2003)

The relationship between the microwave dielectric properties and the IR active phonons of $x\mathrm{Ba}(\mathrm{Mg}_{1/3}\mathrm{Ta}_{2/3})\mathrm{O}_3-(1-x)\mathrm{Ba}(\mathrm{Mg}_{1/3}\mathrm{Nb}_{2/3})\mathrm{O}_3$ ceramics was investigated. The IR modes were assigned, and the origin of dielectric response was determined. Among the 15 prominent IR modes, we found that the normal vibrations of the O layers and that of the Ta/Nb layers are strongly correlated to the measured dispersion parameters, such as the resonant strength ($4\pi\rho$) and the damping coefficient (γ). The frequency shifts of the normal modes of the O layers and that of the Ta/Nb layers explain the linear decrease of microwave dielectric constant (K) as x increases, while the width of these modes correlate with the $Q\times f$ value. © *2003 American Institute of Physics.* [DOI: 10.1063/1.1597969]

I. INTRODUCTION

Complex perovskite compounds with the chemical formula $\mathrm{Ba}(B'_{1/3}B''_{2/3})\mathrm{O}_3$, where $B'=\mathrm{Zn}$, Mg, Ni, or Mn and $B''=\mathrm{Nb}$ or Ta, exhibit ultralow dielectric losses at microwave frequencies,[1–3] when the materials possess $B'-B''$ 1:2 ordered arrangement with a structural symmetry described by the $P\bar{3}m1$ (D^3_{3d}) space group.[4] Since the dielectric properties at microwave range follow mainly from ionic polarization, the phonon vibration spectra of $\mathrm{Ba}(B'_{1/3}B''_{2/3})\mathrm{O}_3$ have been of particular interest.[5–13] H. Tamura *et al.*[5] first analyzed the vibration of 1:2 ordered $\mathrm{Ba}(\mathrm{Zn}_{1/3}\mathrm{Ta}_{2/3})\mathrm{O}_3$ normal modes, and Siny *et al.*[6] investigated the Raman spectra of several complex perovskites, proposing the existence of short-range 1:1 order in $\mathrm{Ba}(\mathrm{Mg}_{1/3}\mathrm{Ta}_{2/3})\mathrm{O}_3$. Recently, the Raman phonons in $\mathrm{Ba}(\mathrm{Mg}_{1/3}\mathrm{Ta}_{2/3})\mathrm{O}_3-\mathrm{Ba}(\mathrm{Mg}_{1/3}\mathrm{Nb}_{2/3})\mathrm{O}_3$ materials were clearly identified.[7]

Ionic sizes and the quality of 1:2 ordered structure are two important parameters that impact the vibration characteristics obtained by Fourier transform infrared (FTIR) spectroscopy. They thus determine the dielectric properties in the microwave region.[7–13] Based on the observation of simple perovskite $Pm3m$ structures,[14,15] the FTIR spectrum of complex perovskite with 1:2 long-range order can be divided into three regimes: (i) frequencies around 150 cm^{-1} correspond to the vibration between the cation and the BO_6 octahedron; (ii) intermediate bands at 150–500 cm^{-1} are mostly related to the B–O stretching mode, and (iii) high-frequency bands above 500 cm^{-1} are correlated with the O–B–O bending mode. The distortion of the BO_6 octahedron in complex perovskite causes the triple-degenerate vibration mode (F mode) in simple perovskite to split into a double degenerate and a non-degenerate modes (E and A modes). However, the normal modes have not yet been assigned to resonant peaks in FTIR spectra, due to the lack of on-site information, such as bonding strength.

This study investigates the FTIR spectra of $x\mathrm{Ba}(\mathrm{Mg}_{1/3}\mathrm{Ta}_{2/3})\mathrm{O}_3-(1-x)\mathrm{Ba}(\mathrm{Mg}_{1/3}\mathrm{Nb}_{2/3})\mathrm{O}_3$ [referred to hereafter as xBMT–$(1-x)$BMN], and its relationship with microwave properties. xBMT–$(1-x)$BMN samples have a complete isostructure, subsequently, the change in IR mode associated with the substitution of Nb ions by Ta ions can be systematically examined. Phonon properties were analyzed for assigning the normal modes and to correlate with microwave dielectric properties.

II. EXPERIMENTS

xBMT–$(1-x)$BMN ceramic samples with $x=0$, 0.25, 0.5, 0.75, and 1 were prepared by a conventional mixed oxide process, in conjunction with a hot isostatic pressing technique. These samples were first conventionally sintered at 1580 °C in air and then hot-isostatically pressed in a 99.9% Ar atmosphere using a Mo chamber. Far-infrared and mid-infrared reflectance spectra were obtained at room temperature using a Bruker IFS 66v FTIR spectrometer. The modulated light beam from the spectrometer was focused onto either the sample or an Au reference mirror, and the reflected beam was directed onto a 4.2-K bolometer detector (40–600 cm^{-1}) and a B-doped Si photoconductor (450–4000 cm^{-1}). The different sources, beam splitters, and detectors used in these studies provided substantial spectral overlap, and the reflectance mismatch between adjacent spectral ranges was less than 1%. The optical properties were calculated from a Kramers-Kronig analysis of the reflectance data.[14] These transformations are performed by extrapolating the reflectance at both low and high frequencies. The low-frequency extensions were determined by using the Lorentz model. Ex-

a)Electronic mail: chiact@phy.ntnu.edu.tw

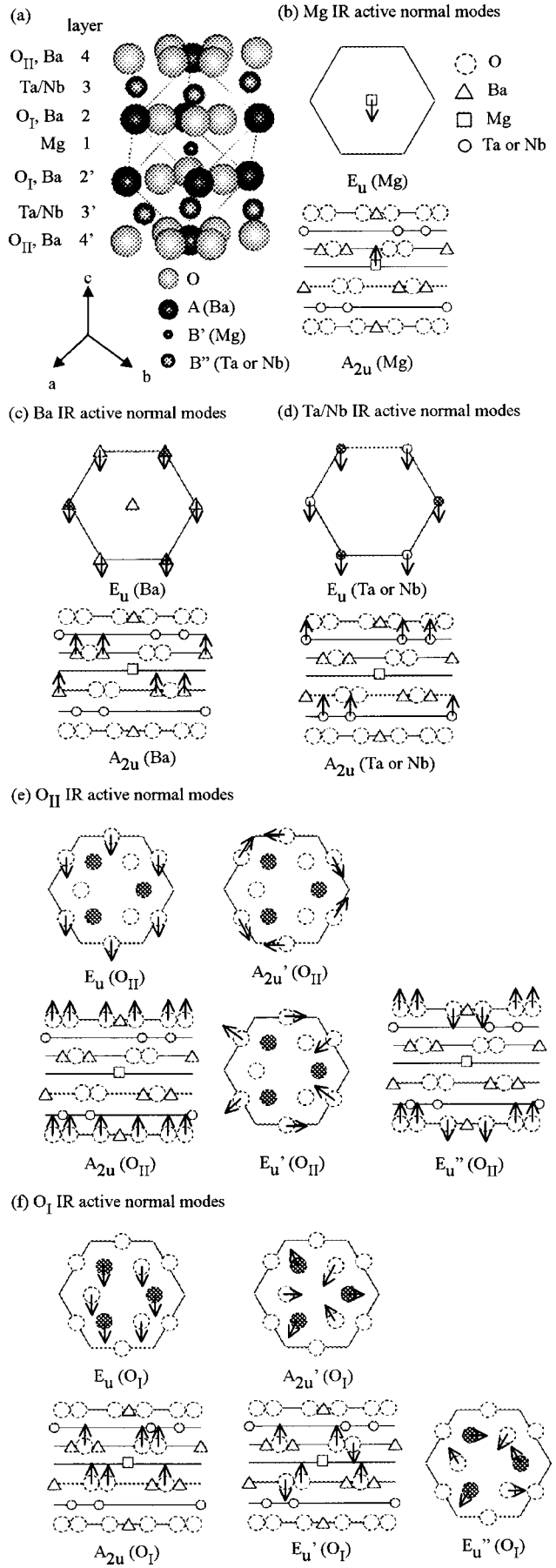

FIG. 1. (a) Crystal structure of $A(B'_{1/3}B''_{2/3})O_3$ complex perovskite. The normal vibration modes of (b) the Mg layer, (c) the Ba layer, (d) Ta/Nb layer, (e) O_{II} layer and (f) O_I layer are depicted.

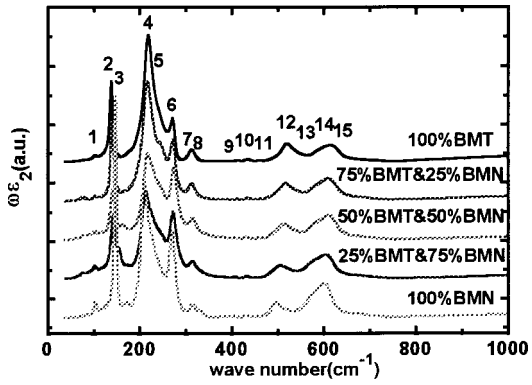

FIG. 2. The dielectric dispersion $\omega\varepsilon_2$ of xBMT–$(1-x)$BMN, with $x=0$, 0.25, 0.5, 0.75, and 1.0.

trapolations to high frequency were made by assuming a weak power law dependence, $R\sim\omega^{-s}$, with $s\sim1-2$.

III. RESULTS AND DISCUSSION

A. Vibration modes

Dielectric properties at microwave frequencies ($\omega_{0j}^2 \gg \omega^2$) can be calculated using dispersion functions[14]

$$\varepsilon_1=\varepsilon_\infty+\sum_j\left(\frac{4\pi e^2N_j}{mV}\right)\cdot\frac{1}{\omega_{0j}^2}=\varepsilon_\infty+\sum_j 4\pi\rho_j, \tag{1}$$

$$\frac{1}{Q}=\sum_j \tan\delta_j=\sum_i\frac{4\pi\rho_j\gamma_j\omega}{\omega_{0j}^2\varepsilon_1}, \tag{2}$$

where ε represents the dielectric constant; N_j and γ_j are the number of charges bound with the resonators of the frequency ω_{0j} and the associated damping coefficient, respectively; m is mass, and V is volume. The summation is over the j modes in the spectrum. The relationship between resonant strength ($4\pi\rho_j$) and resonance frequency (ω_{0j}) originates from the ionic bonding strength and the displacements of the ions. In Eq. (2), the inverse of the quality factor Q equals the dielectric loss ($\tan\delta$), and $Q\times\omega$ is a constant under the $\omega_{0j}^2\gg\omega^2$ approximation at microwave frequencies.

Each vibration mode observed in the FTIR spectra must be identified unambiguously before the microwave dielectric response of the materials can be correlated with the corresponding part of FTIR spectrum. The symmetry of 1:2 ordered $Ba(Mg_{1/3}Ta_{2/3})O_3$ and $Ba(Mg_{1/3}Nb_{2/3})O_3$ complex perovskite ceramics is $P\bar{3}m1$ ($\equiv D_{3d}^3$), as depicted in Fig. 1(a). According to the factor group analysis, the normal modes are $4A_{1g}$[Ba,Ta or Nb,O]$+A_{2g}+5E_g$[Ba,Ta or Nb,O]$+2A_{1u}+7A_{2u}$[Ba,Mg,Ta, or Nb,O]$+9E_u$[Ba,Mg,Ta or Nb,O], where $7A_{2u}+9E_u$, as illustrated in Figs. 1(b)–1(f), are IR active. The important parameters of the dispersion function, ω_{0j}, γ_j, and $4\pi\rho_j$ must be extracted from the FTIR measurements to deduce the dielectric response, and then correlate with the microwave properties.

The complex dielectric constant ($\varepsilon=\varepsilon_1+i\varepsilon_2$) in infrared region was first calculated from the measured infrared reflectivity,[16] using the $K-K$ relation.[14] Figure 2 shows the

TABLE I. Dispersion parameters of BMT derived from Lorentz simple harmonic model.

Designation	ω_{0j} (cm^{-1})	γ_j (cm^{-1})	$4\pi\rho_j$	Vibrating atoms
ω_{01}	75.0	5.66	0.462	E_u(Ta or Nb)
ω_{02}	137.3	2.56	3.967	A_{2u}(Ta or Nb)
ω_{03}	150.9	3.59	0.112	E_u(Ba)
ω_{04}	218.1	9.01	7.539	$E_u(O_{II})$
ω_{05}	242.2	17.33	3.593	$A_{2u}(O_{II})$
ω_{06}	271.3	6.39	1.048	E_u(Mg)
ω_{07}	313.2	6.51	0.205	A_{2u}(Ba)
ω_{08}	380.8	12.01	0.033	A_{2u}(Mg)
ω_{09}	412.2	4.91	0.014	O′
ω_{010}	434.6	6.12	0.026	O′
ω_{011}	460.3	8.69	0.013	O′
ω_{012}	518.2	11.50	0.223	$E_u(O_I)$
ω_{013}	536.5	12.24	0.082	O′
ω_{014}	605.2	28.63	0.388	$A_{2u}(O_I)$
ω_{015}	622.0	9.94	0.044	O′

$\omega\varepsilon_2$ dispersion of the xBMT$-(1-x)$BMN materials thus obtained. Notably, all the peaks are the TO modes and satisfy the Lorentz distribution[14]

$$\omega\varepsilon_2 = \sum_j \left(\frac{4\pi e^2 N_j}{mV}\right) \cdot \frac{\gamma_j \omega^2}{(\omega_{0j}^2 - \omega^2)^2 + \gamma_j^2 \omega^2} \tag{3}$$

Only 15 peaks in these spectra are identifiable. One undetected mode is either too weak to be identified or overlaps the other modes. The three dispersion parameters, including the resonance frequency (ω_{0j}), the damping coefficient (γ_j) and the resonant strength ($4\pi\rho_j$) of j mode resonators, were deduced from Fig. 2 and results listed in Table I. Low-frequency modes (ω_{01}, ω_{02}, ω_{03}, ω_{04}, ω_{05}, ω_{06}, and ω_{07}) and two high-frequency bands (ω_{012} and ω_{014}) possessing large $4\pi\rho_j$ values contribute pronouncedly to the dielectric response at microwave frequencies.

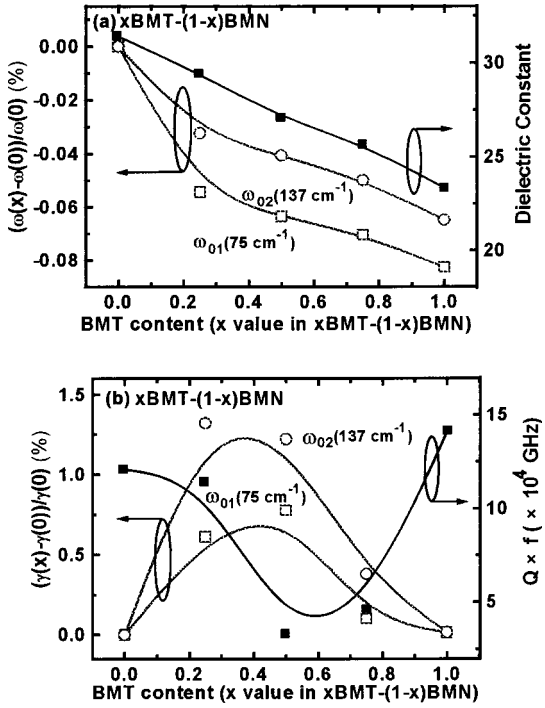

FIG. 3. The microwave dielectric properties of the xBMT$-(1-x)$BMN, and the properties of ω_{01} and ω_{02} modes are plotted as function of x; (a) microwave dielectric constant (K) and frequency-shift ($\Delta\omega/\omega$), and (b) quality factor ($Q\times f$) and damping coefficient ($\Delta\gamma/\gamma$).

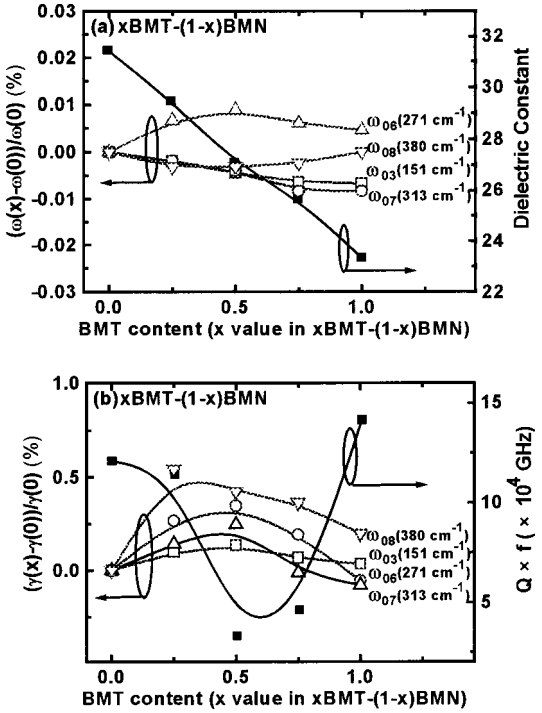

FIG. 4. (a) Microwave dielectric constant (K) of the xBMT$-(1-x)$BMN and frequency shift ($\Delta\omega/\omega$) of ω_{03}, ω_{07}, ω_{06}, and ω_{08} modes, and (b) quality factor ($Q\times f$) of the xBMT$-(1-x)$BMN and damping coefficient ($\Delta\gamma/\gamma$) ω_{03}, ω_{07}, ω_{06} and ω_{08} modes are plotted as function of x.

Each peak in the $\omega\varepsilon_2$ dispersion shows a characteristic frequency shift and width change as x increases, and, accordingly, the normal modes can be classified into three groups. (i) Phonons near 75 cm^{-1} (ω_{01}) and 137 cm^{-1} (ω_{02}), as shown in Fig. 3(a), shift dramatically to lower frequencies as the proportion of BMT (x value) increases (i.e., redshift or softening), and they are designated as R-series phonons. (ii) Phonons at 151 cm^{-1} (ω_{03}), 271 cm^{-1} (ω_{06}), 313 cm^{-1} (ω_{07}), and 380 cm^{-1} (ω_{08}) are relatively invariant with x and are designated as I-series phonons, as shown in Fig. 4(a). (iii) Phonons that harden as x increases (i.e., blueshift modes), are designated as B-series phonons, as presented in Fig. 5(a).

The compositional variation of phonon frequency and linewidth, as well as the resonant strength ($4\pi\rho_j$) listed in Table I, provide important information for identifying normal vibrations. However, a few criteria must to be applied to identify the normal modes and to correlate the vibration modes with the microwave properties. Within the simple harmonic oscillation model, the phonon frequency is approximately proportional to the square root of the force constant between ions and, to the inverse square root of ionic mass. The normal modes that are sensitive to the Ta composition are the vibration of the Ta (or Nb) layer and that of the O layer (cf., Fig. 1). The normal modes associated with the Ta (or Nb) layers are expected to be redshifted. In contrast, sub-

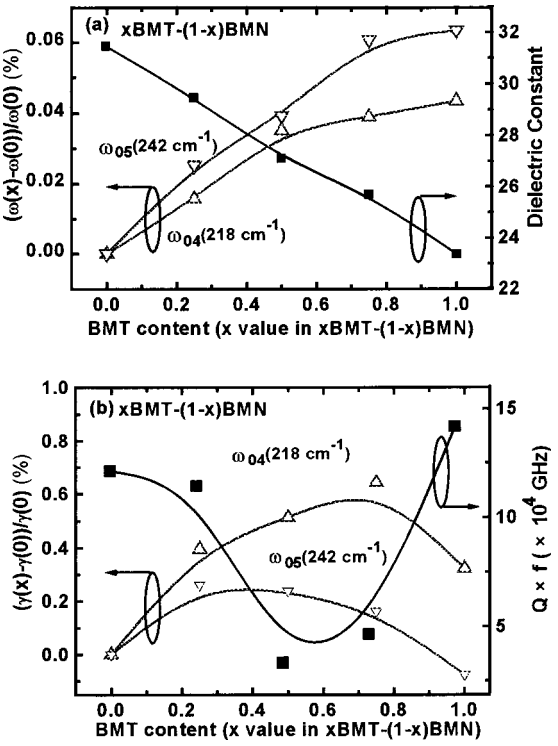

FIG. 5. (a) Microwave dielectric constant (K) of the xBMT$-(1-x)$BMN and frequency shift ($\Delta\omega/\omega$) of ω_{04} and ω_{05} modes, and (b) quality factor ($Q\times f$) of the xBMT$-(1-x)$BMN and damping coefficient ($\Delta\gamma/\gamma$) of the ω_{04} and ω_{05} modes are plotted as function of x.

stituting Ta ions for Nb ions increases the rigidity of the $B''O_6$ octahedron cage, due to relatively large size of the Ta ions; such substitution alters only the force constant of the Ta–O (or Nb–O) bonding of the oxygen octahedral cages. The vibration modes of the O layer are expected to be blue-shifted, as x increases. The line shapes of vibration modes, which involve motion of Ba and Mg atoms, are relatively insensitive to BMT content.

Two R-series phonons, ω_{01} at 75 cm^{-1} and ω_{02} at 137 cm^{-1}, which are shown in Fig. 3(a) and are dramatically redshifted as the concentration of Ta increases, can be assigned to normal modes of the Ta/Nb layer [Fig. 1(d)]. The low-frequency ω_{01} phonon at 75 cm^{-1} is assigned to the E_u mode and the high frequency ω_{02} phonon at 137 cm^{-1} is assigned to the A_{2u} mode, since the frequency of the vibration along the c-axis is known to exceed that of the vibration in the $a-b$ plane; force constant along the c-axis is larger.[17,18]

The normal modes that are relatively insensitive to the Ta/Nb ratio are vibrations of the B'-site lattice (Mg ions) and the A-site lattice (Ba ions), that is, I-series modes. A change in the Ta/Nb ratio can modify the Ba-layer vibration only through changing the lattice constant; this change is small in xBMT$-(1-x)$BMN materials. The normal modes related to the Mg layer are not completely invariant, since increasing the proportion of the TaO_6 octahedron may induce a slight deformation of the octahedron, slightly changing the force constant of the MgO_6 octahedron and thereby slightly modifying the vibration frequency of the Mg layer.

The ω_{06} vibration modes near 271 cm^{-1} shift slightly to higher frequencies as x increases from 0 to 0.5 and then to lower frequencies for $x>0.5$. The ω_{08} vibration modes at 380 cm^{-1} show opposite frequency shifts with respect to Ta concentration. Both can be assigned to the normal vibrations associated with the Mg layer. Furthermore, the low-frequency vibration mode (ω_{06}) is assigned to E_u(Mg), and the high-frequency one (ω_{08}) is assigned to A_{2u}(Mg). ω_{03} and ω_{07} vibration modes at 151 cm^{-1} and 313 cm^{-1}, respectively, which show minimal changes in width and shifts in frequency as x increases, are assigned to Ba-related normal vibrations. Again, the ω_{03}-mode is assigned as E_u(Ba) phonons, whereas the ω_{07}-mode is assigned as A_{2u}(Ba), since the c-axis vibration mode is of high frequency.

Substituting Ta for Nb increases the rigidity of the oxygen octahedron, such that the B-series phonons are blue-shifted. They include ω_{04} at 218 cm^{-1}, ω_{05} at 242 cm^{-1}, ω_{09} at 411 cm^{-1}, ω_{010} at 434 cm^{-1}, ω_{011} at 460 cm^{-1}, ω_{012} at 518 cm^{-1}, ω_{013} at 536 cm^{-1}, ω_{014} at 605 cm^{-1}, and ω_{015} at 622 cm^{-1}, which can be assigned to normal vibrations of the O layers. To clearly identify these phonons, the influence of adjacent layers should be considered.

The unit cell with the 1:2 ordered structure, as shown in Fig. 1(a), has two inner oxygen layers, O_I layers sandwiched between the Mg layer and the Ta/Nb layer, whereas the two outer oxygen layers, O_{II} layers, are adjacent only to the Ta/Nb layers. Normal modes of the O_I layers and normal vibrations of the O_{II} layers are split from F_{1u} and F_{2u} degenerate modes in simple perovskite,[14,15] and can be separated into three pairs, $A_{2u}-E_u$, $A'_{2u}-E'_u$, and $A_{1u}-E''_u$ [Figs. 1(e) and 1(f)]. Of these vibration modes, the normal modes in which the oxygen ions move in phase (such as A_{2u} and E_u modes) should have markedly larger resonant strength ($4\pi\rho$) than the other modes associated with the same oxygen ions, such as A'_{2u} and E'_u modes. Therefore, the former, A_{2u} and E_u modes, can be assigned to ω_{04}, ω_{05}, ω_{012}, and ω_{014}, based on the dispersion parameters listed in the Table I.

"Twisting" octahedron-cage vibrations, associated with the O_I layers, are expected to be of a higher frequency than "shearing motion" of modes associated with the O_{II} layers. Moreover, vibration modes associated with the O_{II} layer are expected to exhibit a larger $4\pi\rho$ than those associated with the O_I layer, because they are adjacent to the Ta/Nb layer. Therefore, ω_{04}, and ω_{05} phonons are assigned as $E_u(O_{II})$ and $A_{2u}(O_{II})$, respectively, as shown in Fig. 1(e). Similarly, two stronger modes, ω_{012} (518 cm^{-1}) and ω_{014} (605 cm^{-1}), in the higher-frequency region are assigned as $E_u(O_I)$ and $A_{2u}(O_I)$ vibrations, respectively, as shown in Fig. 1(f). The vibration modes associated with the O layer exhibit a weak resonance ($4\pi\rho$) because the induced dipole moments are cancelled; these modes are the $A'_{2u}(O)$ and $E'_u(O)$ and $E''_u(O)$ modes. Their resonance is too weak to be clearly identified, and they are thus temporarily designated as O' modes.

Normal vibrations related to O ions also have larger damping coefficients (γ_j) than the others (Table I) because of the vibrations of the O layers that are correlated with the three different oxygen cages: MgO_6, TaO_6, and NbO_6. The coherence of the O-layer vibration is not as high as that of the Ba- (or Mg-) layer vibrations; they are therefore broader.

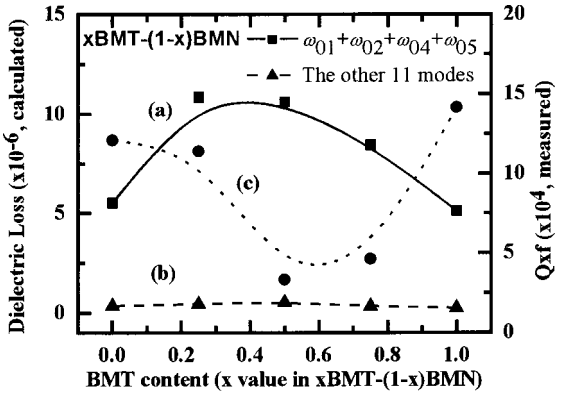

FIG. 6. The calculated dielectric loss $1/Q$ of four dominant normal modes (solid curve) and the measured microwave quality $Q\times f$ at 7 GHz (solid squares) are plotted as function of x.

Table I summarizes the assignment of phonons for BMT–BMN complex perovskite.

B. Microwave dielectric properties

All the infrared active vibration modes presented in Fig. 2 contribute to the microwave dielectric response. The broad vibration modes with large resonance peaks are thus expected to predominate the microwave dielectric properties of xBMT$-(1-x)$BMN [Eq. (2) and Fig. 2]. The normal modes associated with Ta/Nb layer (ω_{01} and ω_{02}) and the normal vibrations of the outer O_{II} layer (ω_{04} and ω_{05}) possess pronouncedly higher resonant strength ($4\pi\rho_j$) and wider width (γ_j) than the other vibration modes (Table I). Therefore, the microwave dielectric properties are predominated by the dielectric responses of ω_{01}, ω_{02}, ω_{04}, and ω_{05}, that is, they are dominated by the normal vibrations of Ta/Nb and O_{II} layers. This argument is supported by the result shown in Fig. 6. The dielectric loss $1/Q$ associated with these four modes, which equals the sum of $4\pi\rho\gamma/\omega_{0j}^2\varepsilon_1$ for ω_{0j} equal to ω_{01}, ω_{02}, ω_{04}, and ω_{05}, is plotted as function of Ta concentration and as the solid curve (a) in Fig. 6, while the calculated $1/Q$ value for the other 11 modes is represented by the dashed curve (b). The experimentally measured quality factor $Q\times f$ is also plotted in solid squares joined by a dotted line (c). Clearly, the $1/Q$ value calculated from ω_{01}, ω_{02}, ω_{04}, and ω_{05} modes dominates dielectric loss in xBMT$-(1-x)$BMN, as found in Fig. 6. The other 11 modes contributed only a little to the dielectric loss. However, the dominant $1/Q$ values of line (a) show a bell-shaped curve, whereas $Q\times f$ are significant for $x=0$ and 1, and is small for $x=0.5$. This finding indicates a strong correlation between normal vibrations of both Ta/Nb and O_{II} layers with the compositional dependence of the measured $Q\times f$ values.

The results presented in Figs. 3, 4, and 5 also support our analysis. Figures 3(a) and 5(a) show compositionally dependent frequency shifts ($\Delta\omega/\omega$) of Ta/Nb-layer modes (ω_{01} and ω_{02}) and O_{II}-layer modes (ω_{04} and ω_{05}). Furthermore, Figs. 3(b) and 5(b) present the variations of the damping coefficients ($\Delta\gamma/\gamma$) with Ta concentration of these predominant modes. Figures 4(a) and 4(b) indicate that the Mg-layer and Ba-layer phonons contribute insignificantly to the microwave dielectric properties, consistent with the fact that these modes have very small resonant strength (cf., Table I and Fig. 2), and only slightly affect the microwave properties of xBMT$-(1-x)$BMN.

Figure 3(a) depicts softening of the normal modes of the Ta/Nb layer and a dielectric function that increases with Ta concentration. These results indicate the strong relationship between dielectric constant and the degree of long-range 1:2 ordered structure. The decrease in dielectric constants (K) with increasing x is accompanied by a blueshift of normal frequencies of the O_{II} layer [Fig. 5(a)]. The blueshift of the O-layer vibration modes caused by increased TaO_6 content in the xBMT$-(1-x)$BMN implies that TaO_6 octahedrons are much more rigid, or the Ta–O bonds are much stronger than the NbO_6(Nb–O) bonds. The dielectric constant (K) of sample that contains high population of TaO_6 octahedrons is small, because the polarizability for rigid oxygen octahedron is small.

In Figs. 3(b) and 5(b), phonon widths ($\Delta\gamma/\gamma$) of normal modes of the O_{II} and Ta/Nb layers are narrowed at the end point compositions, $x=0$ and 1, and are broad at midpoint ($x=0.5$) composition. When Ta ions were added to the $Ba(Mg_{1/3}Nb_{2/3})O_3$ as substitutes for some of the Nb ions, the coherence of normal vibrations of the Nb layers markedly deteriorated and the quality of 1:2 ordered structure was degraded. Similarly, when Nb ions were incorporated into the $Ba(Mg_{1/3}Ta_{2/3})O_3$, the quality of 1:2 ordered structure was degraded. As a result, the damping coefficient (γ_j) increased and the $Q\times f$ value declined, as found in Fig. 3(b) for Ta and Zn atoms coexisting in compounds. Similarly, Fig. 5(b) reveals that randomly mixing TaO_6 /NbO_6 degrades the coherency of the normal modes of the TaO_6 (or NbO_6) octahedron (ω_{04} and ω_{05}), resulting in large damping coefficients (γ) and low $Q\times f$ values for $x=0.5$.

IV. CONCLUSION

xBMT$-(1-x)$BMN ceramics were studied by FTIR spectroscopy. The normal modes were assigned by investigating the frequency shift versus Ta concentration. Microwave dielectric properties are closely correlated with high-intensity modes at low-frequency bands of far infrared spectra. Microwave dielectric constants are strongly related to ω_{01} and ω_{02} that represent the quality of 1:2 ordered structure, and ω_{04} and ω_{05} modes that indicate the rigidity of the three-dimensional oxygen-octahedral network. $Q\times f$ values of xBMT$-(1-x)$BMN are affected by the distortion of the oxygen octahedron, $B''O_6$, and the coherence of the normal vibrations of the Ta/Na layer.

ACKNOWLEDGMENT

The authors would like to thank the National Science Council, Republic of China, for financially supporting this research under Contract Nos. NSC 91-2622-E-007-032, NSC 91-2112-M-003-024, and NSC 92-2218-E-003-001.

[1] S. Nomura, K. Toyama, and K. Kaneta, Jpn. J. Appl. Phys., Part 2 **21**, L642 (1982).
[2] R. Guo, A. S. Shalla, and L. E. Cross, J. Appl. Phys. **75**, 4704 (1994).
[3] S. Nomura, T. Konoike, Y. Sakabe, and K. Wakino, J. Am. Ceram. Soc. **67**, 59 (1984).

[4] F. S. Galasso, in *Structure, Properties and Preparation of Perovskite-Type Compounds* (Pergamon, Oxford, 1969), pp. 13–15, 55.
[5] H. Tamura, D. A. Sagala, and K. Wakino, Jpn. J. Appl. Phys., Part 1 **25**, 787 (1986).
[6] I. G. Siny, R. W. Tao, R. S. Katiyar, R. A. Guo, and A. S. Bhalla, J. Phys. Chem. Solids **59**, 181 (1998).
[7] C. T. Chia, Y. C. Chen, H. F. Cheng, and I. N. Lin, J. Appl. Phys. **94**, 3360 (2003).
[8] H. Tamura, D. A. Sagala, and K. Wakino, J. Am. Ceram. Soc. **76**, 2433 (1993).
[9] K. Tochi and N. Takeuchi, J. Mater. Sci. Lett. **8**, 1144 (1989).
[10] T. Nagai, M. Sugiyama, M. Sando, and K. Nihara, Jpn. J. Appl. Phys., Part 1 **35**, 5163 (1996).
[11] K. Tochi and N. Takeuchi, J. Mater. Sci. Lett. **7**, 1080 (1988).
[12] K. Tochi, N. Takeuchi, and S. Emura, J. Am. Ceram. Soc. **72**, 158 (1989).
[13] N. Sugiyama and T. Nagai, Jpn. J. Appl. Phys., Part 1 **32**, 4360 (1993).
[14] W. G. Spitzer, R. C. Miller, D. A. Kleinman, and L. E. Howarth, Phys. Rev. **126**, 1710 (1962).
[15] A. S. Barker, Jr. and M. Tinham, Phys. Rev. **125**, 1527 (1962).
[16] I. N. Lin, C. T. Chia, H. L. Liu, H. F. Cheng, and C. C. Chi, Jpn. J. Appl. Phys., Part 1 **41**, 6952 (2002).
[17] M.-L. Hu, C.-T. Chia, J. Y. Chang, W.-S. Tse, and J.-T. Yu, Mater. Chem. Phys. **78**, 358 (2003).
[18] J. D. Freire and R. S. Katiyar, Phys. Rev. B **37**, 2074 (1988).